Microstructure- and property-controllable NdAlNiCuFe alloys by varying Fe content

Z. Zhang, D.Q. Zhao, and W.H. Wang[a)]
Institute of Physics, Chinese Academy of Sciences, Beijing 100080, China

We report the formation of microstructure- and property-controllable $Nd_{60}Al_{10}Ni_{10}Cu_{20-x}Fe_x$ ($0 \leq x \leq 20$) alloys by varying the content of Fe element. The microstructure of the Nd-based alloy can be changed progressively from a full glassy state into a composite state with nanocrystalline particles in the glassy matrix and, finally, into a nanostructured state, accompanied by variation in magnetic property gradually from paramagnetic to hard magnetic. The role of Fe addition in the control of microstructure and magnetic property is clarified. We expect that the results would have implication in the development of the microstructure- and property-controllable functional materials for various applications.

I. INTRODUCTION

Microstructure- and property-controllable alloys are expected to be used in a variety of technological contexts. However, the microstructural control in the metallic alloys is a longstanding problem due to the high nucleation and growth rates and instability of their supercooled liquid state. Bulk metallic glass (BMG)-forming alloys with a very stable supercooled liquid state and high thermal stability against crystallization[1,2] offer a large experimentally accessible time and temperature window for developing some methods, such as controlled solidification,[3,4] high annealing,[5,6] and pressure,[7] to control their microstructure and properties through controlling of the nucleation and growth in supercooled liquid state. The rare-earth (RE)-metal-based alloys have attracted intensive attention due to their high glass-forming ability (GFA), and anomalous magnetic properties.[8–12] For Nd-based alloys, it was reported that the bulk glass rod with 12 mm diameter can be obtained by suction casting into a copper mold.[7] However, the Nd-based BMGs actually are regarded as a type of clustered amorphous material. Direct evidences are that the BMGs have no obvious glass transition in their differential scanning calorimeter (DSC) traces as other BMGs have done and exhibit hard magnetic, while ribbons with the same composition are magnetically soft.[9–11]

In our previous work, we found that element addition is an effective way to influence the GFA, properties, and microstructure of the BMG-forming alloys.[13–19] Fe content is found to have a significant effect on the magnetic properties and GFA of the Nd-based alloys.[8–10] Therefore, it is possible to control the microstructure and magnetic properties of the Nd-based alloys by Fe addition. In this paper, we report the formation of full bulk glassy $Nd_{60}Al_{10}Ni_{10}Cu_{20}$ alloy. Based on the BMG, the microstructure and property are manipulated in the alloy by controlling additional Fe content. By varying Fe content, the microstructure of the Nd-based alloy changes progressively from full glassy state to composite state with nanocrystalline particles in the glassy matrix, and finally changes into a nanostructured state, accompanying the magnetic property changes gradually from paramagnetic to hard magnetic. The role of Fe content in the controlling of microstructure and magnetic properties is clarified.

II. EXPERIMENTS AND METHODS

$Nd_{60}Al_{10}Ni_{10}Cu_{20-x}Fe_x$ ($0 \leq x \leq 20$) ingots were prepared by melting pure (99.9%) Nd, Al, Ni, Cu, and Fe elements in an arc-melting furnace under argon atmosphere. Cylinders of 3 to 5 mm diameters and 80 mm length were produced by suction or cast of the melt into a copper mold. The sample rods were cut into slices, and the cut surfaces were used for x-ray diffraction (XRD) experiments. XRD data of the alloys containing different Fe contents were analyzed by using a MAC M03 XHF (MAC Inc., Japan) diffractometer with Cu K_α radiation. DSC measurements were carried out in a Perkin Elmer DSC-7 (Perkin Elmer Inc., USA) with a temperature scanning rate of 20 K/min^{-1}. High-resolution transmission

electron microscopy (HRTEM) observation was performed in a JEOL-2010 (JEOL Inc., Japan) operating at 200 kV. Magnetic properties were carried out on a Physical Properties Measurement System (PPMS, Quantum Design Co., USA).

III. RESULTS AND DISCUSSION

The XRD patterns of the $Nd_{60}Al_{10}Ni_{10}Cu_{20-x}Fe_x$ alloys with different Fe contents ($0 \leqslant x \leqslant 20$ at.%) prepared by the Cu mold-casting method are shown in Fig. 1. For comparison, all sample rods are 3 mm in diameter. For the alloy without Fe addition, the XRD pattern shows a broad maximum peak followed by a lesser-intensity broad peak, and no appreciable diffraction peaks corresponding to crystalline phase can be seen. This indicates the as-cast rod consists only of an amorphous phase. The $Nd_{60}Al_{10}Ni_{10}Cu_{20}$ alloy can be cast into full amorphous up to 5 mm in diameter. Unlike other Nd-based alloys, its XRD pattern is similar to that of Zr-based BMGs.[1–4] The $Nd_{60}Al_{10}Ni_{10}Cu_{20-x}Fe_x$ alloys with Fe content less than 10 at.% also exhibit typical broad amorphous peaks within the resolution limit of the XRD. However, the intensity of the two diffused peaks increases, suggesting that its microstructure varies with Fe content changing. For the alloy with 15% Fe, some broad and weak crystalline peaks superimpose in the XRD curve, indicating the mixture microstructure of the nanocrystalline and amorphous phases. When Fe content is larger than 15%, the broader crystalline peaks appear, indicating the alloys consist mainly of nanocrystalline phases. The precipitation crystalline phases are identified as ferromagnetic Nd, Nd_2Fe_{17}, and other unknown intermetallics (as marked in Fig. 1),[20] which are responsible for the high coercivity observed in the alloys.[10] The XRD result indicates that the Nd-based alloys show a pronounced degradation trend of GFA, and their microstructure changes progressively from full glassy state to composite state with nanocrystalline phase in glassy matrix, and finally changes into a nanostructured state with increasing Fe content. We have prepared alloys using various methods, such as die casting, suction casting, and melt spinning. Each method has a different cooling rate. The alloys with the same Fe content demonstrate similar glass formability regardless of the cooling rate. This implies that the microstructural change tendency is not sensitive to the cooling rate.
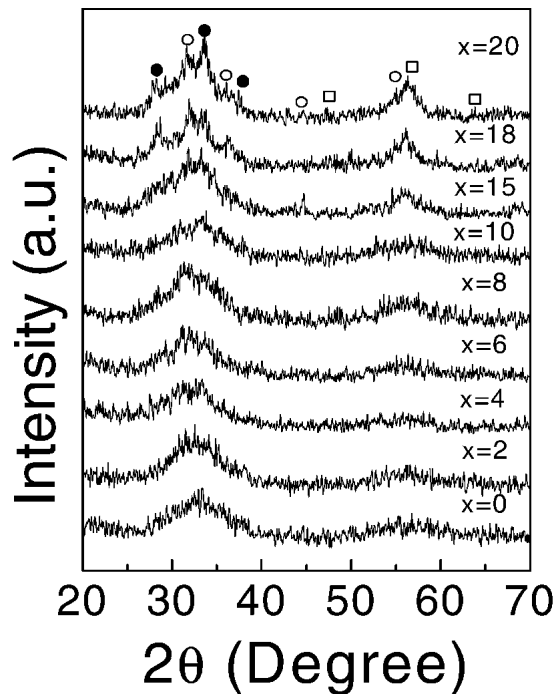
The crystallizations of the $Nd_{60}Al_{10}Ni_{10}Cu_{20-x}Fe_x$ ($0 \leqslant x \leqslant 20$) alloys measured by DSC with a constant heating rate of 20 K/min are shown in Fig. 2. The DSC results also exhibit the microstructural change upon Fe content. The glass transition temperature, T_g, the onset temperatures of the first crystallization, T_{x1}, and the supercooled liquid region, $\Delta T = T_{x1} - T_g$, for these alloys are listed in Table I. Unlike other RE-based BMGs,[8–11] the remarkable features of the DSC trace of the $Nd_{60}Al_{10}Ni_{10}Cu_{20}$ alloy are an obvious broad endothermic peak before crystallization, demonstrating a distinct glass transition with onset at $T_g = 438$ K and a large

FIG. 1. XRD patterns for the as-cast $Nd_{60}Al_{10}Ni_{10}Cu_{20-x}Fe_x$ (x = 0, 2, 4, 6, 8, 10, 15, 18, 20) alloys. The marks in the figure indicate the ferromagnetic Nd (●), Nd_2Fe_{17} (○), and other unknown intermetallics (□).
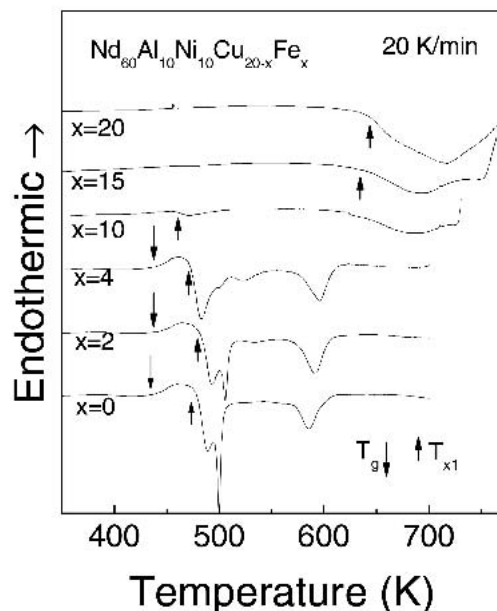
FIG. 2. DSC curves show the crystallization process of $Nd_{60}Al_{10}Ni_{10}Cu_{20-x}Fe_x$ (x = 0, 2, 4, 10, 15, 20) alloys at a heating rate of 20 K/min.

TABLE I. The crystallization temperatures (T_{x1}, T_{x2}), glass transition temperature (T_g), supercooled liquid region (ΔT), melting temperature (T_m), liquidus temperature (T_l) and reduced glass transition temperature (T_{rg}) for $Nd_{60}Al_{10}Ni_{10}Cu_{20-x}Fe_x$ ($0 \leqslant x \leqslant 20$) alloys.

Fe at.%	T_g (K)	T_{x1} (K)	T_{x2} (K)	ΔT (K)	T_{rg}	T_m (K)	T_l (K)
0	438	478	572	40	0.60	728	755
2	442	482	573	40	0.60	723	765
4	436	472	578	34	0.60	713	755
10	421	455	598	34	0.58	726	776
15	⋯	640	⋯	⋯	⋯	760	780
20	⋯	653	⋯	⋯	⋯	786	823

$\Delta T = 40$ K. Two sharp exothermic crystallization events occur with onset at $T_{x1} = 478$ K and $T_{x2} = 572$ K. The features of the distinct glass transition, sharp crystallization events of the DSC trace for the alloy, are similar to those of other typical BMGs[1] and further confirm the full glassy state of the NdAlNiCu BMG. It is worth noting that the T_g of the BMG is very low among the known BMGs.[1,23] The excellent glass-forming ability and low T_g may give the BMG significant potential in applications such as phase change erasable optical storage.[24] For the alloys $x = 2$ and 4, their DSC traces also show obvious glass transition and crystallization. However, the crystallization enthalpy decreases with increased Fe addition, indicating a decrease in the amorphous fraction in the alloy. For the alloy $x = 10$, no obvious glass transition and only a tiny exothermic peak are found, while a very broad exothermal peak corresponding to the growth of the nanocrystalline clusters[25] can be seen in the DSC trace. For Fe-rich ($x = 15$, 20) samples, no glass transition and sharp crystallization peaks are found in their DSC traces, while the broad peak becomes more pronounced, indicating only the growth of nanocrystalline phase occurs upon heating for the alloys. The broad exothermal peaks in the DSC curve is a common feature of RE–Fe–Al alloys (RE = Nd, Pr, Y, Sm), which is attributed to the growth of the nanocrystalline phase.[8–11] The DSC results confirm that the alloys with higher Fe content are nanocrystalline alloy.

The HRTEM pictures for the representative $Nd_{60}Al_{10}Ni_{10}Cu_{20-x}Fe_x$ alloys (x = 0, 4, and 20) are shown in Fig. 3. For the Fe-free alloy, the HRTEM picture and the inset diffraction halo in Fig. 3(a) exhibit no obvious crystalline clusters, confirming the full glassy structure of the alloy. However, when Fe content increases up to 4%, nanoclusters with average size of 5 nm can be clearly seen arbitrarily and uniformly distributed in the glassy matrix, demonstrating the composite state with nanocrystalline particles of the alloy [Fig. 3(b)]. However, both the size and the volume fraction of the nanoparticles are too small to be detected by XRD. For the alloy with $x = 20$, the picture and the diffraction

rings in Fig. 3(c) show that the alloy consisting mainly of heterogeneous and disoriented nano-ordered regions with an average size of approximately 8 nm is nanocrystalline alloy. The composite microstructure of the alloy is similar to that of the known $Nd_{60}Al_{10}Fe_{20}Co_{10}$ alloy.[26] HRTEM results confirm further that Fe addition induces microstructural change from glass state to nanocrystalline state.

Figure 4 shows the melting process of the $Nd_{60}Al_{10}Ni_{10}Cu_{20-x}Fe_x$ alloys upon Fe content. The values of melting temperature, T_m, liquidus temperature, T_l, and reduced glass transition temperature ($T_{rg} = T_g/T_m$) for the alloys are also listed in Table I. As shown in Fig. 4 and Table I, both the melting process and the value of T_m are sensitive to Fe content. For the Fe-free alloy, the melting point is near eutectic temperature, indicating the alloy is of the composition near the eutectic composition. The best glass-forming composition for an alloy is usually near deep eutectic composition, where the melt can be cooled to the underlying T_g with the smaller temperature interval.[27] Thus, the T_{rg} is a critical parameter for determining the GFA of an alloy. For the Fe-free alloy, T_{rg} is approximately 0.6, which classifies it as a highly glass-forming alloy.[27] With increasing Fe content, on one hand, one can see that the melting point of the alloy is gradually deviate from eutectic point, and the GFA is degraded. On the other hand, according to the "confusion principle,"[28] the alloys with five components have much higher viscosity in the supercooled liquid compared with conventional metallic melts. The growth of the crystalline phases in the viscous melt is very difficult,[1] causing the nanocrystalline particles to precipitate. The formation of fine nanocrystalline observed in Fe-rich alloys could also be related to phase separation in the undercooled liquid, which is a common phenomenon in the bulk glass-forming alloys.[1] The origin of phase separation in the Nd–Fe–Al system may be attributed to the heat of mixing the two main components of Nd and Fe,[29] which is positive (+1 kJ/mol).[30] The mutually repulsive interaction between Nd and Fe leads to clustering in amorphous alloys prepared by continuous cooling from liquid state; the clustering or phase separation already present in the liquid state is frozen in alloys.[31]

The room temperature M-H hysteresis loops measured at a maximum applied field of 2000 kAm^{-1} for the $Nd_{60}Al_{10}Ni_{10}Cu_{20-x}Fe_x$ alloys are shown in Fig. 5. The change of the coercivity of the alloys as a function of Fe content is shown in the inset in Fig. 5. The alloy without Fe addition shows paramagnetic at room temperature. With Fe addition, the coercivity increases from 0 to 276 kA/m for the alloy with $x = 20$, indicating a hard magnetic property of the alloy. The value is close to that of the $Nd_{60}Al_{10}Fe_{20}Co_{10}$ hard magnetic BMG.[8–11] The values of saturation magnetization M_s and remanence M_r also increase with increasing Fe content as shown in
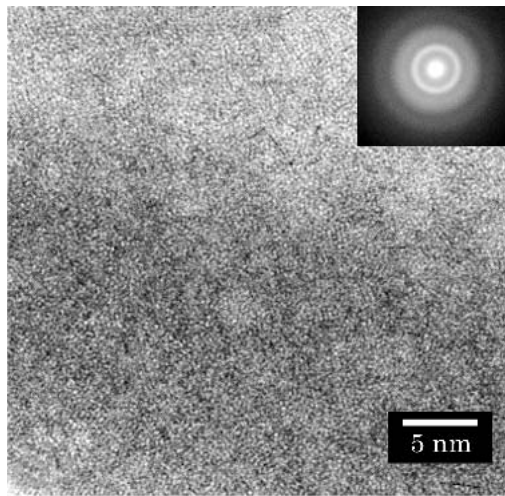
(a)
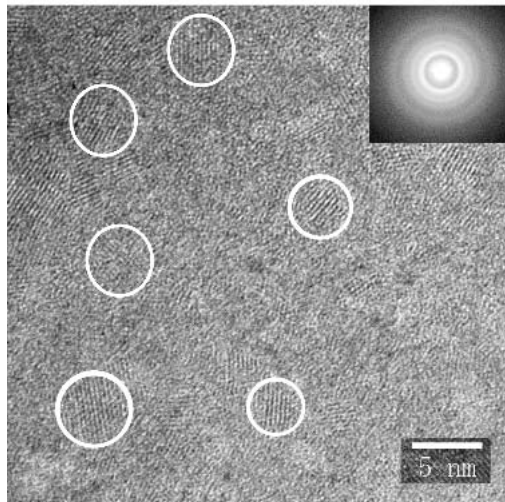
(b)
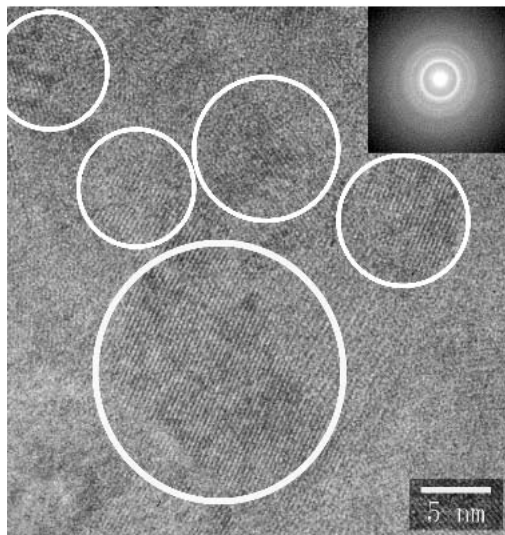
(c)

FIG. 3. High-resolution TEM image of the as-cast $Nd_{60}Al_{10}Ni_{10}Cu_{20-x}Fe_x$ ($x = 0, 4, 20$) alloys: (a) alloy with $x = 0$, (b) alloy with $x = 4$, and (c) alloy with $x = 20$.
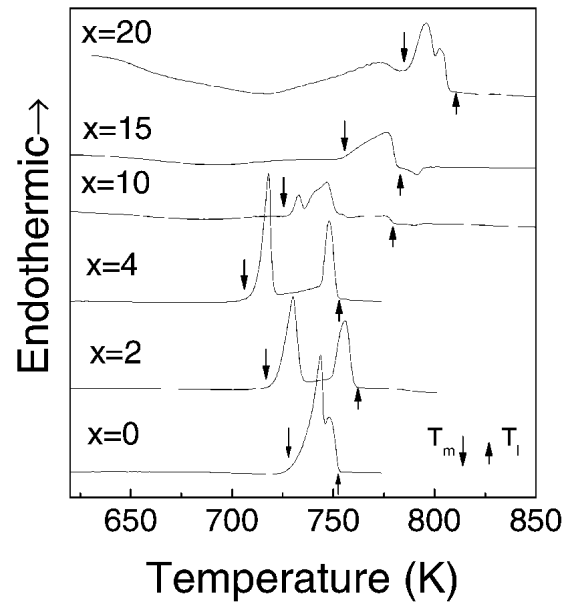
FIG. 4. DSC curves show the melting process of $Nd_{60}Al_{10}Ni_{10}Cu_{20-x}Fe_x$ ($x = 0, 2, 4, 10, 15, 20$) alloys at a heating rate of 20 K/min.
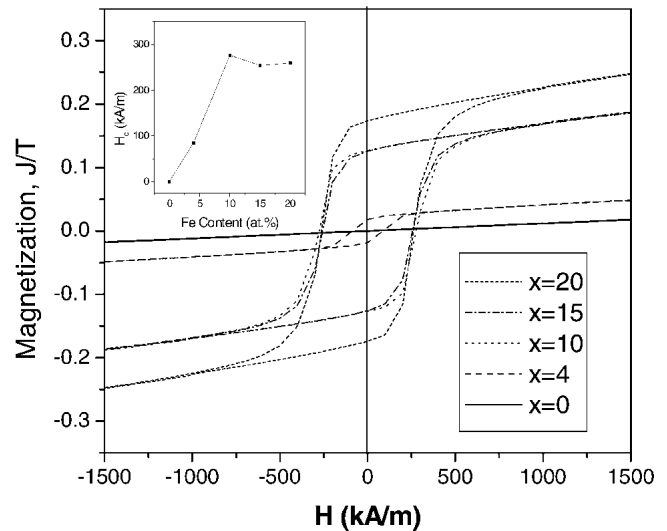
FIG. 5. Hysteresis M-H loops of the as-cast $Nd_{60}Al_{10}Ni_{10}Cu_{20-x}Fe_x$ ($x = 0, 4, 10, 15, 20$) alloys. The inset shows the variation of coercivity as a function of Fe content.

Fig. 5. The results indicate that the property of the Nd-based alloys changes progressively from paramagnetic to hard magnetic with the increase of Fe content.

The understanding of the correlation between the measured magnetic properties and the possible magnetic phases are very important, and a number of works on this topic have been published.[31–36] To clarify the correlation, however, more work is necessary. Our Fe addition results may be useful for understanding the origin of the observed hard magnetic behavior in Re-based alloys. The hard magnetic properties of the Nd-based alloys can be

correlated to the pre-existence nanocrystalline phase,[11] which is so small it cannot be detected by XRD. The clusters with approximate composition of Fe_3Nd (A_1 phase), Nd, and Nd_2Fe_{17} are possibly responsible for the coercivity observed in the nanoclustered Nd-based alloys.[20,31,32] The magnetic exchange coupling interaction among the magnetic clusters with large random anisotropy causes the high coercivity of the homogeneous magnetic system.[11,30] For the Fe-free alloy and the alloy with poor Fe content, the size of the clusters are small and the magnetic ordering temperature is lower than room temperature. Under these conditions the magnetic moment of each particle is not fixed but fluctuates rapidly and results in paramagnetic behavior at room temperature. With more Fe addition, the moment of the large particles arranges more orderly, the magnetization stiffness increases, and the magnetic ordering temperature is increased with the formation of larger nanoparticles. This is an important underlying cause for the increase in coercivity with further Fe addition.

IV. CONCLUSION

The $Nd_{60}Al_{10}Ni_{10}Cu_{20}$ BMG with a very low glass transition temperature and stable supercooled liquid state is obtained. By varying Fe content, the microstructure of the $Nd_{60}Al_{10}Ni_{10}Cu_{20}$ alloy changes progressively from full glassy state to composite state with nanocrystalline particles in the glassy matrix, and finally changes into nanostructured state, accompanying the structural evolution from glass to nanostructured state, and the magnetic property changes gradually from paramagnetic to hard magnetic. The role of Fe content in the controlling of the microstructure, magnetic properties, and GFA of the alloys is attributed to the formation of nanocrystalline Nd, Fe–Nd compounds, which result from the Fe addition induced phase separation and GFA degradation in the alloys.

ACKNOWLEDGMENTS

REFERENCES

1. W.L. Johnson: Bulk glass-forming metallic alloys: Sciences and technology. *MRS Bull.* **24** (10), 24 (1999).
2. W.H. Wang, C. Dong, C.H. Shek: Bulk metallic glasses. *Mater. Sci. Eng. R.* **44,** 45 (2004).
3. W.H. Guo, F.F. Chua, C.C. Leung, and H.W. Kui: Formation of bulk nanostructured materials by rapid solidification. *J. Mater. Res.* **15,** 1605 (2000).
4. W.H. Guo and H.W. Kui: Bulk nanostructured alloy formation with controllable grain size. *Acta Mater.* **48,** 2117 (2000).
5. W. Liu and W.L. Johnson: Precipitation of bcc nanocrystals in bulk Mg-Cu-Y amorphous alloys. *J. Mater. Res.* **11,** 2388 (1996).
6. W.H. Wang, R.J. Wang, W.T. Yang, D.Q. Zhao, and M.X. Pan: Stability of supercooled liquid state of ZrTiCuNiBe bulk metallic glass forming alloy. *J. Mater. Res.* **17,** 1385 (2002).
7. W.H. Wang, D.W. He, D.Q. Zhao, Y.S. Yao, and M. He: Nanocrystallization in ZrTiCuNiBeC bulk metallic glass under high pressure. *Appl. Phys. Lett.* **75,** 2770 (1999).
8. Y. He, C.E. Price, and S.J. Poon: Formation of Nd-based metallic glasses. *Philos. Mag. Lett.* **70,** 371 (1994).
9. A. Inoue, A. Takeuchi, and T. Zhang: Bulk glass forming based on rare earth elements. *Metall. Mater. Trans.* **29A,** 1779 (1998).
10. G.J. Fan, W. Löser, S. Roth, and J. Eckert: Glass-forming ability of RE–Al–TM alloys (RE = Sm, Y; TM = Fe, Co, Cu). *Acta. Mater.* **48,** 3823 (2000).
11. B.C. Wei, W.H. Wang, M.X. Pan, B.S. Han, and W.R. Hu: $Nd_{65}Al_{10}Fe_{25-x}Co_x$ bulk metallic glasses with wide supercooled liquid regions. *Phys. Rev. B.* **64,** 012406 (2001).
12. Z.F. Zhao, Z. Zhang, P. Wen, M.X. Pan, D.Q. Zhao, Z. Zhang, and W.H. Wang: Highly glass forming alloy with very low glass transition temperature. *Appl. Phys. Lett.* **82,** 4699 (2003).
13. W.H. Wang, Q. Wei, and H.Y. Bai: Enhanced thermal stability and microhardness in metallic glass ZrTiCuNiBe alloys by carbon addition. *Appl. Phys. Lett.* **71,** 58 (1997).
14. Z. Bian, R.J. Wang, M.X. Pan, D.Q. Zhao, and W.H. Wang: Excellent wave absorption ability of Zr-based bulk metallic glass composites containing carbon nanotubes. *Adv. Mater.* **15,** 616 (2003).
15. W.H. Wang, Z. Bian, P. Wen, Y. Zhang, and M.X. Pan: Role of addition in formation and properties of Zr-based bulk metallic glasses. *Intermetallics* **10,** 1249 (2002).
16. Y. Zhang, D.Q. Zhao, and W.H. Wang: Formation ZrNiCuAl bulk metallic glasses with low purity elements. *Mater. Trans.* **41,** 1410 (2000).
17. W.H. Wang, R.J. Wang, G.J. Fan, and J. Eckert: Formation and properties of Zr-(Ti, Nb)-Cu-Ni-Al bulk metallic glasses. *Mater. Trans.* **42,** 587 (2001).
18. Y. Hu, M.X. Pan, L. Liu, and W.H. Wang: Synthesis of Fe-based bulk metallic glasses with low purity materials by multi-metalloids addition. *Mater. Lett.* **57,** 2698 (2003).
19. W.H. Wang, M.X. Pan, D.Q. Zhao, and H.Y. Bai: Enhance soft magnetic properties of FeCoZrMoWB bulk metallic glass by microalloying. *J. Phys.: Condens. Matter* **16,** 3719 (2004).
20. Z.G. Zhao, F.R. de Boer, and K.H.L. Buschow: Magnetic properties of $R_6Fe_{11}A_{13}$ and $R_6Fe_{12}A_{12}$ compounds with R = Pr, Nd. *J. Alloys and Compd.* **239,** 147 (1996).
21. B. Grieb and E. Henig: The ternary NdAlFe system. *Z. Metallkede* **82,** 560 (1991).
22. D.Q. Zhao, W.H. Wang: Melting and crystallization of $Nd_{60}A_{110}Fe_{20}Co_{10}$ bulk metallic glass under high pressure. *J. Phys.: Condens. Matter* **15,** L749 (2003).
23. W.H. Wang, L.L. Li, M.X. Pan, and R.J. Wang: Characteristics of glass transition and supercooled liquid state of $Zr_{41}Ti_{14}Cu_{12.5}Ni_{10}Be_{22.5}$ bulk metallic glass. *Phys. Rev. B* **63,** 052204 (2001).
24. M. Libera and M. Chen: Phase change erasable optical storage. *MRS Bull.* **15,** 40 (1990).
25. H.J. Fecht: Thermodynamic properties of amorphous solids—glass formation and glass transition. *Mater. Trans. JIM.* **36,** 777 (1995).

318

J. Mater. Res., Vol. 20, No. 2, Feb 2005

26. Z. Zhang, L. Xia, B.C. Wei, D.Q. Zhao, M.X. Pan, and W.H. Wang: Structural evolution and property changes in $Nd_{60}Al_{10}Fe_{20}Co_{10}$ bulk metallic glass during crystallization. *Appl. Phys. Lett.* **81,** 4371 (2002).

27. D. Turnbull: Under what conditions can a glass be formed? *Contemp. Phys.* **10,** 473 (1969).

28. A.L. Greer: Confusion by design. *Nature* **366,** 303 (1993).

29. Z.G. Sun, W. Löser, J. Eckert, and L. Schultz: Phase separation in $Nd_{60-x}Y_xFe_{30}Al_{10}$ melt-spun ribbons. *Appl. Phys. Lett.* **80,** 772 (2002).

30. F.R. De Boer, R. Boom, W.C.M. Mattens, A.R. Miedema, and A.K. Niessen: *Cohesion in Metals* (North-Holland, Amsterdam, 1988).

31. J. Delamare, D. Lemarchand, and P.J. Vigier: Structural investigation of the metastable compound A1 in an as-cast Fe–Nd eutectic alloy. *J. Alloys Compd.* **216,** 273 (1994).

32. V.P. Menushenkov, A.S. Lileev, M.A. Oreshkin, and S.A. Zhuravlev: Metastable nanocrystalline A_1 phase and coercivity in Fe–Nd alloys. *J Magn. Magn. Mater.* **203,** 149 (1999).

33. G.J. Fan, W. Löser, S. Roth, J. Eckert, and L. Schultz: Magnetic properties of cast $Nd_{60-x}Fe_{20}Al_{10}Co_{10}Cu_x$ alloys. *Appl. Phys. Lett.* **75,** 2984 (1999).

34. M.J. Kramer, A.S. O'Connor, K.W. Dennis, R.W. McCallum, L.H. Lewis, L.D. Tung, and N.P. Duong: The origins of coercivity in the amorphous alloy NdFeAl. *IEEE Trans. Magn.* **37,** 2497 (2001).

35. I. Betancourt and R. Valenzuela: The role of cluster formation on the magnetic properties of NdAlFe-based magnetic alloys. *J. Mater. Res.* **27,** 427 (2003).

36. G. Kumar, J. Eckert, S. Roth, W. Stefan, W. Löser, and L. Schultz: Structural and magnetic properties of as-cast Nd-(Fe,Co)-Al alloys (*Annales de Chimie,* Paris, France), **27,** 41 (2002).

J. Mater. Res., Vol. 20, No. 2, Feb 2005

319